Chapter 18
Optical Standards and Measurement

18.1 Introduction

The early development of lasers was marked not only by the explosive proliferation of laser oscillation on different atomic and molecular transitions, but also by efforts to stabilize them and narrow their spectral line width. This was driven by the realization that the very attribute that makes the laser so remarkable is the one that still left room for spectacular improvement: spectral purity. The fundamental quantum limit on spectral purity far exceeds that of any common laser subject to fluctuations in its optical cavity. As we saw in the example given in Chapter 14, the theoretical spectral line width of a 1mW laser with a 1m long cavity is on the order of 3×10^{-4} Hz, or a fractional line width of 5×10^{-19}!

Considerable early success was achieved in reducing "artificial" broadening of a laser output by mode selection techniques and servo phase-locking the laser to a resonant mode in a mechanically isolated external cavity with high finesse. In order to achieve long term frequency stability however, a narrow atomic or molecular resonance was sought whose frequency falls within the tuning range of the laser, to serve as a reference to servo-control the laser frequency. A striking example is the classic work on the stabilization of the infra-red line of the He-Ne laser using the saturated absorption method on a resonance line in methane gas. This made possible a number of important applications: from high-resolution interferometry to detect continental drift and seismic waves, to high-resolution spectroscopy.

With the development of a number of highly stabilized lasers having frequencies dotting the spectrum from the far infrared to the visible, and nonlinear devices effective in that frequency range to generate harmonics and combine frequencies, it became within the realm of possibility to actually measure the frequency of a light wave. This would have been an unimaginable prospect prior to the laser, and it is still far from a simple matter, involving advanced laser techniques. Until recently, only the *wavelength* of such radiation could be measured; and it is only since the advances we shall be considering in this chapter

F.G. Major, The Quantum Beat

that it has become useful to describe radiation in terms of its frequency. One now speaks, for example, of the CO_2 laser ($\lambda = 10.6\ \mu m$) as having a frequency around 28.3 THz (1 terahertz = 1000 GHz). This extension of the capability of measuring frequency to the optical regime requires special techniques to generate ultrahigh order harmonic frequencies, spanning the wide gulf between the microwave primary standard and optical frequencies. A number of stabilized lasers, including HCN, H_2O, CO_2, Ne, and Ar^+ are available for the purpose of providing in effect intermediate secondary standards to form frequency chains.

Recently the whole field of optical frequency measurement has been taken to a new level of sophistication through two developments: (1) the observation of ultrasharp optical transitions from long-lived metastable states in laser-cooled single ions frozen in rf microtraps, and (2) the ability to generate coherent "frequency combs" consisting of coherent equally spaced sideband frequencies above and below a central carrier optical frequency stretching so far as to span almost a full octave, reaching the microwave region of the Cs standard.

18.2 Definition of the Meter in Terms of the Second

The effort to measure optical frequencies has been spurred by the adoption in 1983 of a new definition of the unit of length, the meter. It had been felt for some time that the relativistically invariant scale factor between time and space coordinates, the velocity of light, could be *defined* to have a particular value, thereby enabling the unit of distance to be defined in terms of the much more accurately kept unit of time. This came to pass at the 17^{th} General Conference on Weights and Measures, which adopted the definition of the meter as "... the length of the path traveled by light *in vacuo* in 1/299, 792, 458 of a second." This means that the velocity of light is now *by definition* exactly 299, 792, 458 m/s, the number being chosen, of course, so that the new meter is very nearly equal to the old standard. As a matter of principle, the new definition recognizes the relativistic point of view that space and time are not absolute and separate concepts; and as a practical matter, a standard of time interval (or frequency) can be maintained and measured with vastly greater accuracy than the distance between two points. Moreover, all distance measurements based on radar methods, and this includes all aerospace and much of interplanetary measurements, are in fact propagation times for electromagnetic waves of one wavelength or another. Previously, the unit of length was defined in terms of the wavelength of a certain line in the spectrum of krypton gas. With the new definition of the meter, the measurement of distance between two points is reduced ultimately to counting the number wavelengths of radiation of measured frequency contained in that distance. It follows that for the greatest precision, the wavelength used for this purpose should be as short as possible; hence the need for the measurement of frequency of radiation extending to the optical region of the spectrum.

18.3 Secondary Optical Frequency Standards

18.3.1 Saturated Absorption

As with the microwave standards, the discovery of suitable reference atomic/molecular transitions and the methods of eliminating factors that broaden their frequency width parallel the study of high-resolution spectroscopy, and its drive to observe spectra under conditions of the utmost spectral resolution and accuracy. The reference transition should occur between quantum states whose (spontaneous) radiative lifetime is adequately long to allow a long interrogation time and hence a sharp resonance. Also, the frequency of that resonance should be well separated from neighboring resonances and be relatively insensitive to environmental conditions such as ambient temperature and electromagnetic fields. In the days prior to the development of advanced techniques for synthesizing different wavelengths of coherent laser light, these were formidable conditions to fulfill, considering that suitable lasers with narrow spectral output are few in number and tended to have limited tunability. The best chance of satisfying them is in the rich spectra of molecules, spectra that characteristically consist of *bands*, each made up of closely spaced lines spanning a range of wavelengths. Moreover, there is almost a limitless variety of molecules, a far greater number than atomic species. To avoid spectral broadening due to intermolecular forces, the molecules should make up a low-pressure gas. The challenge is then to reach the resolution permitted by the natural line width of the absorber in the inevitable presence of a much wider Doppler broadening due to thermal motion. There have in the past been many approaches to defeating the ever-present Doppler effect. The most direct way of reducing the Doppler effect is of course by cooling the particles. Other techniques that have been developed to achieve sub-Doppler line widths are saturated absorption (or fluorescence); two-photon absorption, and Ramsey separated fields, with which we are familiar.

Great success has been achieved, as we have already seen, in the case of stabilizing a diode laser against a resonance in atomic Cs as reference, using *saturated absorption* from two counter-propagating parallel laser beams, tuned to resonance with the desired atomic transition. Only atoms having a nearly *zero* velocity component along the beam axis are *simultaneously* resonant with both laser beams; any other molecules will see two field frequencies Doppler-shifted in opposite directions. The action of the combined beams can result in such a high rate of absorption that a significant number are in the excited state, leaving a depletion of the number in the absorbing ground state. This marks the onset of *saturation* in the amount of absorption: the gas becomes more transparent. It is important to distinguish between this process in which each molecule absorbs only *one* photon at a time (but at a higher rate), from another *two-photon* technique for achieving sub-Doppler line widths, which we will encounter later.

18.3.2 Stabilization of He–Ne laser lines

One of the earliest attempts at stabilizing the output frequency of a laser with respect to a molecular resonance was on the helium–neon laser, because, as a gaseous laser, it has an inherently narrower spectral width than other types of lasers. However, because it can be tuned only over a very narrow range, it is necessary to find a species of atom or molecule that fortuitously has a transition that can be resonantly induced by the laser radiation. There are two molecular species that have been exploited with enormous success: one is the hydrocarbon methane (CH_4), otherwise known by the unglamorous name of "marsh gas," and the other is molecular iodine vapor (I_2). We recall that the He–Ne laser can generate not only the familiar red light at $\lambda = 633$ nm, but also radiation in the near infrared at $\lambda = 3.39\,\mu$m; which wavelength dominates can be controlled by the design and operating conditions of the laser. It happens that certain lines in the spectra of CH_4 and I_2 fall within the narrow tuning range of the He–Ne laser operating at $\lambda = 3.39\,\mu$m and 633 nm respectively.

We will consider some details of the use of methane to stabilize a He-Ne laser mainly for its historical interest. At ordinary temperatures methane is a gas consisting of molecules each made up of one central carbon nucleus surrounded by four hydrogen nuclei (protons) at the corners of a regular tetrahedron, all immersed in a cloud of electrons that holds the molecule together through chemical bonds, as shown in Figure 18.1 The quantum energy states between which transitions resonate with the He–Ne output at 3.39 μm are ones that differ both with respect to vibration of the nuclei with respect to each other and rotation of the molecule as a

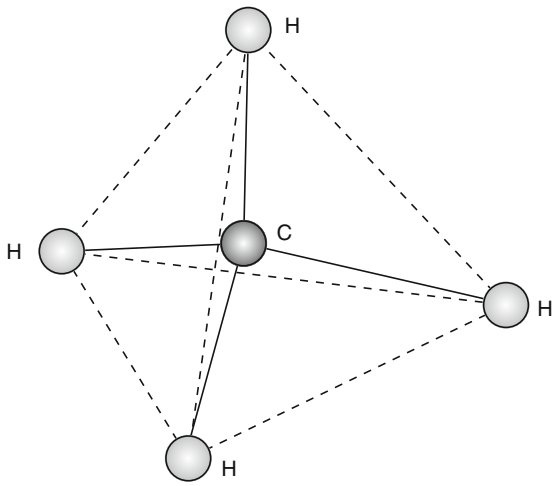

Figure 18.1 The symmetry of the methane (CH_4) molecule

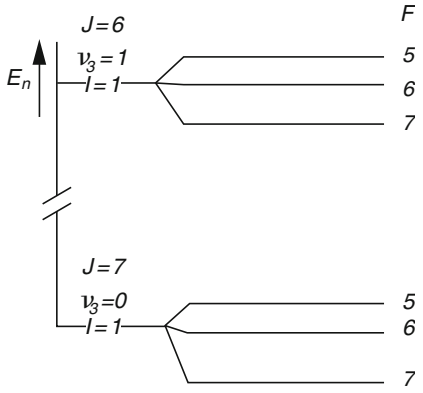

Figure 18.2 The vibration–rotational levels in CH_4 relevant to the stabilization of the He–Ne laser

whole, as shown schematically in Figure 18.2. The states are grouped according to vibrational quantum number but are differentiated within each group according to their angular momentum.

We see that the angular momentum quantum number (J) can reach fairly large values. Transitions in which $J' - J = -1$ are conventionally classified as forming the P-branch of the spectrum; similarly, those in which $J' - J = +1$ form the R-branch. The specific transition that can be made resonant with the $\lambda = 3.39\ \mu m$ output of the laser is in the fine structure of what is designated as the P(7) component in the $\nu_3 = 0 \rightarrow \nu_3 = 1$ characteristic vibration band, in which $J = 7 \rightarrow J = 6$.

The physical setup of the saturated absorption system for stabilizing a He–Ne laser consists essentially of a chamber several meters long containing methane gas at low pressure, provided with infrared transmitting windows. Beam-expanding optics and a retroreflector are provided to ensure precisely parallel counterpropagating laser beams passing through the gas. The return beam intensity is monitored with an infrared detector, such as a cooled In–Sb photoconductive detector. If the laser frequency is swept across the resonant frequency, there is a sharp peak in the intensity of the return beam, which can be used to derive an error signal for the servo control of the laser. The apparatus is shown schematically in Figure 18.3.

There are several factors that may limit the attainable sharpness of the resonance, and hence the tightness of control of the laser frequency. The most serious is the finite interaction time as the molecules cross the laser beams with their thermal velocity: The other factors have to do with the parallelism of the reflected beam with the forward beam, and their angular divergence; these lead to (first-order) Doppler shifts in the resonance of a molecule moving across the beams. There is a fundamental lower limit on the divergence set by diffraction, which can be lowered only by widening the aperture. At the level of spectral resolution

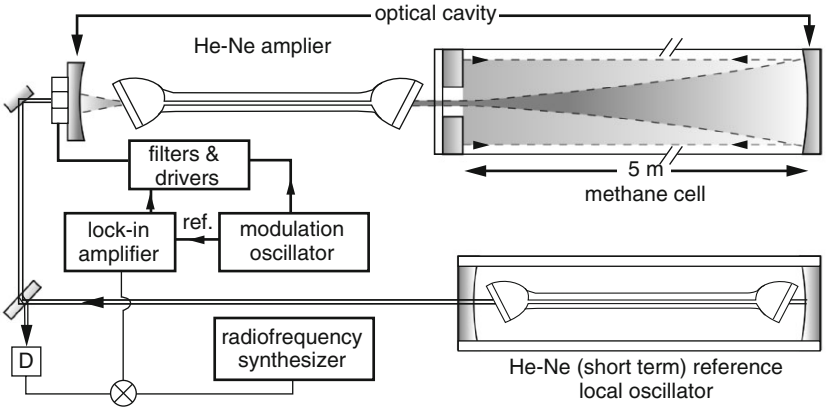

Figure 18.3 Experimental arrangement for laser stabilization using saturated absorption in methane gas

involved here, amounting to only a few hundred hertz in a frequency of 10^{14}, many other subtle sources of spectral broadening and frequency shifts become significant. These include the second-order Doppler effect, broadening and shift due to collisions between molecules; and Zeeman broadening in Earth's magnetic field.

For the familiar red beam at $\lambda = 633$ nm generated by a He–Ne laser, the reference transition is a hyperfine component in the visible part of the band spectrum of molecular iodine I_2. At room temperature, iodine is a solid with a relatively high vapor pressure, which reaches around 100 Pa at 38°C. The stable isotope has mass number 127 and a nuclear spin of $5/2$, giving rise to a hyperfine structure in a rich spectrum containing a high density of lines in the $\lambda = 500\,\text{nm} - 670\,\text{nm}$ range.

As a diatomic molecule, the classification of its energy levels is a good deal simpler than that for methane. It has, of course, only one mode of vibration and two equal principal moments of inertia perpendicular to the molecular I–I axis. The curves showing the mutual potential energy of the two iodine nuclei as a function of their distance apart, an amount of energy arrived at approximately by solving for the electron energy states corresponding to fixed nuclei, are shown in Figure 18.4 for the ground state and the first excited electronic state. In the neighborhood of the points where the potential is minimum, the shape of the curves is parabolic, as for a simple harmonic oscillator. Thus within each electronic state there is an array of vibrational energy levels represented by the horizontal lines, and each of these is further split into closely spaced levels of rotational energy. According to the *Franck-Condon Principle*, in a quantum transition from one electronic state to another, the effect on the nuclear motion is negligibly small, and thus transitions are represented by vertical lines between points at which the kinetic energy is the same for the two electronic states.

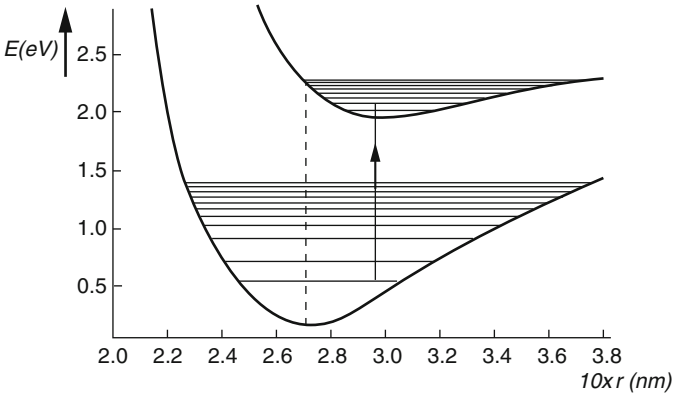

Figure 18.4 The molecular potential curves for the iodine molecule I_2 relevant to the stabilization of the He–Ne laser

As with methane, saturated absorption is used to obtain sub-Doppler resolution in stabilizing the He–Ne laser line using an electronic transition in I_2 vapor. In principle, the same basic design considerations, such as beam expansion to increase transit time across the beam, wave front curvature, and beam alignment are equally important here as in the methane case. In practice, however, because the I_2 line resonant with the He–Ne $\lambda = 633$ nm light is weak, the absorption cell containing the iodine vapor is placed *inside* the laser cavity to interact with the intense optical field there. This circumstance has detracted from the accuracy and resetability that can be achieved in practice. Nevertheless, it has been widely used as a laboratory standard of wavelength, since it surpasses the standard krypton lamp.

18.3.3 Stabilization of the CO_2 Laser

Another type of laser which, suitably stabilized, plays an important role in providing a reference frequency, is the carbon dioxide (CO_2) laser, which operates in the infrared around 10.6 μm (28.3 THz).

It is unique in allowing a useful saturation *fluorescence* signal from CO_2 itself to be used for stabilization. The frequencies of lasing transitions in several isotopes, such as $^{12}C^{16}O_2$ and $^{13}C^{18}O_2$, have been measured to almost 1 part in 10^{10}. There are altogether some 600 CO_2 frequencies that can serve as secondary standards in the infrared. Unfortunately, the reproducibility is ultimately limited by pressure shifts in the frequency of the CO_2 cell used for stabilization. The spectra of other molecular candidates for stabilization of the CO_2 laser have been studied; the most promising is osmium tetroxide, OsO_4, with which accuracies in the neighborhood of parts in 10^{12} have been achieved.

18.3.4 Stabilization Using Two-Photon Transitions

In the stabilized laser systems so far discussed, sub-Doppler line widths were achieved in the reference molecular resonance by the saturated absorption (or fluorescence) method, in which each molecule absorbs *one* photon from counterpropagating laser beams. (Simultaneous resonance with both beams simply increases the probability of absorbing that one photon, in a given time.) But another important technique for achieving Doppler-free line widths, which has been exploited in the context of optical frequency standards, involves the simultaneous absorption by each atom or molecule of *two photons* from counterpropagating beams. Although the probability of such a two-photon process is vastly smaller than that for the one photon process, nevertheless, it can be significant with sufficient laser power and a favorable disposition of the quantum levels of the absorber. It had long been observed in magnetic resonance experiments at microwave and radio frequencies, where strong coherent fields have been readily available; however, it is only after the advent of the laser that it has become feasible to observe them at infrared and optical frequencies. To understand the way in which the Doppler effect is rendered ineffective in broadening the resonant absorption, suppose ν_0 is the frequency of the reference transition in a molecule placed in two counterpropagating laser beams of frequency ν_L. If the molecule has a component of velocity V in the direction of the common beam axis, then it will see the frequencies of the two beams Doppler shifted to $\nu_L(1 + V/c)$ and $\nu_L(1 - V/c)$. Now, the simultaneous absorption of two photons, one photon from each of the two beams, results in the molecule gaining an amount of energy $2h\nu_L$, no matter what its velocity happens to be; and therefore resonance will occur at $2\nu_L = \nu_0$ for *all* molecules. The quantum selection rules that govern two-photon transitions are naturally different from those of the usual one-photon process; in particular, the angular momentum of the initial and final states and their dependence on the polarization of the photons. If the two beams have the same polarization, then it is possible that two-photon absorptions occur from the *same* beam, in which case absorption can occur at Doppler-shifted frequencies by groups of molecules having different corresponding velocities. This would lead to a resonance line shape with a Doppler-broadened base on which is superposed a sharp Doppler-free peak. It is possible to eliminate the Doppler base if the two counter-propagating beams have different polarizations (for example, right and left circular polarizations) and the quantum selection rules applied to the given transition allow only one photon from each beam.

As an example of the application of this technique in the context of optical frequency standards we describe briefly the work reported in 1994 by the group at the LPTF, in collaboration with other groups in France (Touahri et al., 1994), on the stabilization of a GaAlAs diode laser using two-photon transitions in the rubidium atom. In Figure 18.5 is shown a partial energy level diagram of the Rb atom, for which the two lower energy states are already familiar from the optical pumping of the Rb standard. The two-photon transition is between the $5^2S_{1/2}$ ground

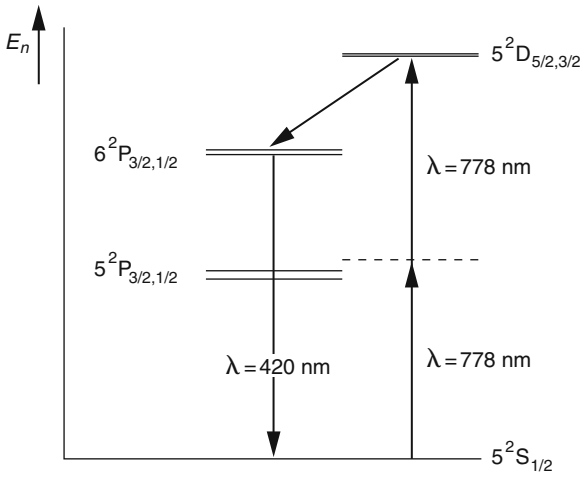

Figure 18.5 Partial energy diagram of Rb showing the 2-photon 5S–5D transition and the intermediate 5P level

state and the $5^2D_{1/2}$ excited state. Such a transition is *forbidden* in a one-photon (dipole) process; however, a two-photon process, although generally expected to be improbable, is in this particular case greatly enhanced by the presence of a level $5^2P_{1/2}$ approximately midway between the initial and final levels. This intermediate level is only 1.05 THz from the exact middle position The sequence of events following the simultaneous absorption of two photons is that the atom is raised to the upper 5D state from which it quickly cascades down by allowed one-photon transitions, first to the 6P state and then emits a photon in the blue region of the spectrum at $\lambda = 420.2$ nm. in making a strong transition to the 5S ground state. The emission of the blue line is eminently suitable for detecting the occurrence of two-photon transitions. Not only does it appear if and only if this two-photon transition has been induced, but it lies in a region of the spectrum where photomultipliers have low dark current, and so far removed from the laser frequency that spurious background scattering of the laser light is easily filtered out. We recall that the Rb spectrum contains many hyperfine components, and with the high spectral resolution implicit in all the techniques we are concerned with, the laser is stabilized on a particular hyperfine resonance. The general layout is shown schematically in Figure 18.6. The diode laser is in an *extended cavity* in which spectral narrowing is achieved by having a diffraction grating forming one of the reflectors, whose angle is servo-controlled along with the diode current to obtain a frequency lock. The rubidium vapor absorption cell is placed in an external cavity, allowing for the control of the power and alignment of the counter-propagating beams. The laser frequency is modulated at 70 kHz, and the blue fluorescence is detected with a photomultiplier whose output signal goes to a lock-in amplifier in which

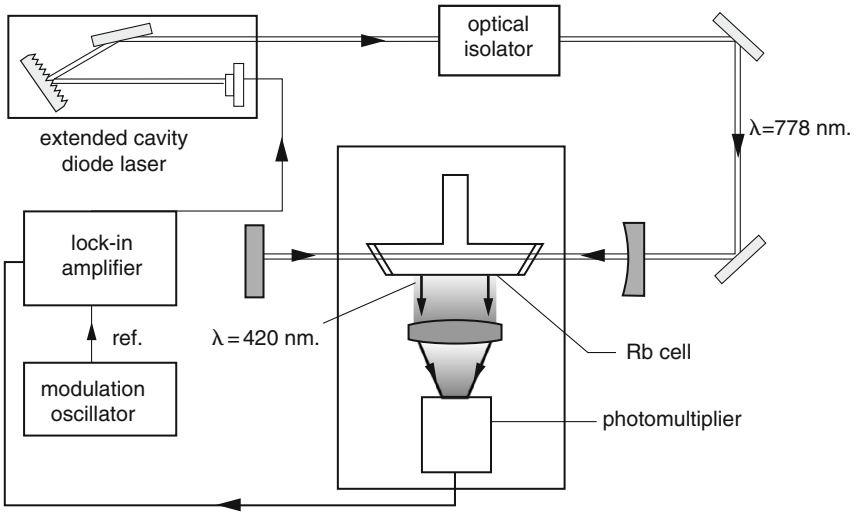

Figure 18.6 Schematic diagram of apparatus for 2-photon resonance in Rb to stabilize GaAlAs diode laser

the modulation frequency serves as reference. The output of the lock-in amplifier is the error signal used to servo-control the laser system. The frequency stability reported of a few parts in 10^{14} for an integration time of 300 seconds is an order of magnitude better than has been achieved with a He–Ne laser stabilized using I_2 as a reference. The largest correction is the light shift, which amounts to about one part in 10^{11}. However, it is relatively well understood, and extrapolation to zero light intensity is good enough to make this system competitive with the stabilized He–Ne/I_2 system.

18.4 Optical Standards Based on Laser Cooled Ions

18.4.1 The $^{199}Hg^{+}$ Ion Optical Standard

The degree of sophistication in laser techniques and ion confinement in miniature electric fields has reached the point of making it possible to observe transitions of extraordinarily narrow spectral width at *optical frequencies* in single ions frozen in a trap. To take advantage of the long unperturbed observation time, an optical frequency "clock" transition must be chosen to be an intrinsically narrow one between long-lived states; this requirement is met by what are referred to as metastable excited states, since the only possible transitions from them to the ground state are "forbidden" in the electric dipole approximation and only the higher order quadrupole transitions are allowed. Thus in $^{199}Hg^{+}$ one such transition is between a

metastable $^2D_{5/2}$ state with the orbital angular momentum quantum number $L = 2$ and the ground state $^2S_{1/2}$ with $L = 0$. A transition for which $L_2 - L_1 = 2$ has zero probability in the dipole approximation, but a small but finite probability in the next higher order, that is the electric quadrupole approximation.

Several mainly national standards laboratories are pursuing the development of optical frequency standards based on a variety of ion species: for example, NIST (USA) on the ion $^{199}Hg^+$, NRC (Canada) and NPL (Britain) on $^{88}Sr^+$, PTB (Germany) and NPL on $^{171}Yb^+$, and Max Plank Inst. für Quantenoptik. (Germany) on $^{115}In^+$. It is apparent from the diversity of ion species chosen by the different groups that the nascent field of optical clocks is undergoing an evolutionary process which will ultimately lead to the adoption of a particular ion species to redefine the unit of time in the future. The accuracy and precision of optical standards have already matched the best Cs fountain clock, and there is little doubt that they will eventually supersede the Cs microwave standard.

While the various groups are pursuing different ion species, the essential design of these various systems is very similar; therefore we will attempt a broad "generic" description of optical clock development and not be overly burdened with the minutiae of experimental details that in fact often test the ingenuity of researchers in the laboratory. Our description may be framed in terms of one group's project for the sake of clarity, by specifying concrete devices and procedures, but it must be understood that essentially the same is true of the other projects.

Therefore we begin with a brief description in terms of the $^{199}Hg^+$ optical clock developed at NIST, since it has been advanced to the point of operating as a clock over an extended period. A diagram of the relevant energy levels of $^{199}Hg^+$ is shown in Figure 18.7. The optical frequency reference is chosen to be

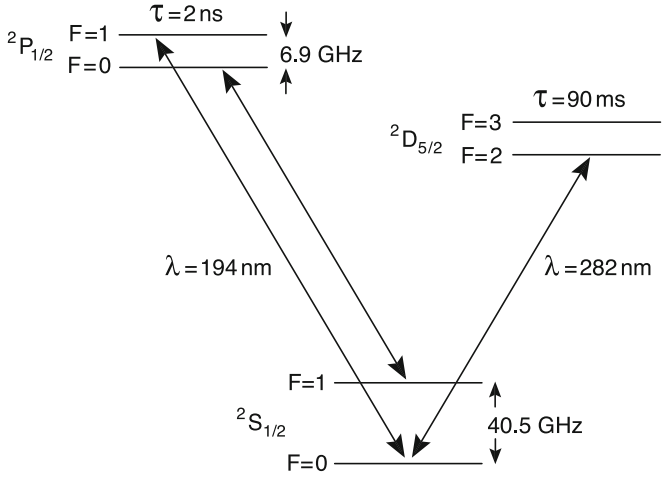

Figure 18.7 Relevant energy levels of $^{199}Hg^+$

that of the weak electric quadrupole transition $^2S_{1/2}(F = 0, m_F = 0) \rightarrow {}^2D_{5/2}$ $(F = 2, m_F = 0)$ having a natural linewidth of about 2 Hz at a frequency of 1.06×10^{15} Hz corresponding to a theoretical line Q $\approx 5 \times 10^{14}$! The wavelength of this transition at $\lambda = 282$ nm is in the ultraviolet region of the spectrum, so the main experimental challenge in realizing this degree of spectral resolution, of course, is to synthesize laser radiation at this wavelength with an extraordinary degree of spectral purity, compatible with the spectral width of the transition.

Furthermore, in order to realize in practice the ultra-narrow *natural* linewidth of the ion just quoted requires, of course, that all sources of line broadening be eliminated. This begins first by eliminating collisions with background particles, second providing a proper magnetic field environment, and third, laser cooling the ion to eliminate Doppler broadening. The central focus around which the whole system is designed is a single ion confined typically in some version of a miniaturized Paul trap, which might be a limiting form of the Paul quadrupole trap consisting of a small ring, and two "end caps" which may in fact be some form of conductors symmetrically positioned on the axis on either side of the ring. As in the microwave standard described in the last chapter, the $^{199}Hg^+$ optical standard of the Boulder group makes use of cryogenic pumping at liquid helium temperature to freeze out residual background particles in the space around the trap. The trap is mounted in a copper vacuum chamber held approximately at a temperature of 4 K inside a nested liquid He-liquid nitrogen cryostat. This eliminates collisions with background mercury vapor and other gases which may cause frequency shifts, shields the ion from external magnetic fields with the same salutary effect, and extends the lifetime of the ion in the trap to about 100 days!

Laser cooling of the ion begins in the *Doppler cooling* regime to a limit of about 1.7 mK. However it will be recalled that with a suitably designed "strong" miniature trap with a secular ion oscillation frequency sufficiently large that the Doppler sidebands are well resolved, it is possible to continue the cooling with a single laser to reach the Lamb-Dicke regime and ultimately the zero point energy in the trap, in the microkelvin range of temperatures. The transition used to cool the ion is a hyperfine component of the strong ion resonance line at 194 nm corresponding to the transition $^2S_{1/2}(F = 1) \rightarrow {}^2P_{1/2}(F = 0)$, while another beam repumps on the hyperfine component $^2S_{1/2}(F = 0) \rightarrow {}^2P_{1/2}(F = 1)$ to counteract the optical pumping of the ion into the non-absorbing $^2S_{1/2}(F = 0)$ state by the cooling transitions. The 194 nm laser frequency is synthesized from the sum of two frequencies at 257 nm and 792 nm in a nonlinear crystal as was also described in the last chapter.

The intricate sequence of operations on the different laser beams involved in probing the clock transition is coordinated using synchronously operated electro-optic light shutters. First the ion is cooled using both hyperfine resonance frequencies at $\lambda = 194$ nm, then pumped into the $^2S_{1/2}(S = 0)$ state by stopping the repumping component, and finally the $\lambda = 194$ nm beam is blocked while the ion

is interrogated with the stable $\lambda = 282$ nm beam for about 50 ms. The interrogation time should theoretically extend to the full lifetime of the metastable state for maximum resolution. The occurrence of clock transitions to the metastable state is detected using the optical double resonance (the so-called "electron shelving") technique, in which the strong resonance fluorescence at $\lambda = 194$ nm enables a nearly 100% efficient detection of whether a clock transition has occurred.

The synthesis of the clock transition wavelength at $\lambda = 282$ nm can be accomplished by frequency doubling the output of a highly stabilized dye or solid state laser operating at twice the wavelength at $\lambda = 563$ nm. The laser is first prestabilized by being locked to a high finesse ($F \approx 800$) Fabry–Pérot cavity using the *Pound-Drever-Hall* technique described in Chapter 14. Feedback signals control the laser separately with respect to long term drift, and with respect to the short term noise using an electro-optic modulator in the laser cavity. This prestabilization results in a narrowing of the laser output linewidth to about 1 kHz. An optical fiber is used to connect the output of the laser to a second ultrahigh finesse ($F \approx 200{,}000$) Fabry–Pérot cavity mounted on a thermally and mechanically isolated table. Again the Pound-Drever-Hall method is used to provide high and low frequency corrections, this time to the prestabilization *cavity*.

The stabilization of the laser with reference to a cavity transfers the burden of achieving high stability to the cavity itself. There are three critical sources of possible instability: (1) temperature fluctuations causing changes in cavity dimensions (2) mechanical vibrations and (3) possible refractive index changes due to residual intracavity scattering by residual particles. The first source of instability is minimized by the choice of materials. The NIST group used a low expansion titania silicate glass developed by Corning for NASA (with NASA funding, no doubt) that goes under the trademark name ULE (ultra-low expansion). This is the material of the critical spacer separating the two mirrors of the cavity, a solid cylinder 25 cm in length and 15 cm in outer diameter with a 1 cm hole drilled along the axis, and a radial hole to the axis to allow evacuation of the intracavity space. The cavity is supported inside a vacuum chamber, the temperature of which is stabilized at around 30°C , at the point where the temperature coefficient of ULE is zero. The chamber is mounted on a passively stabilized optical table mechanically isolated by being suspended by 3 m strands of surgical tubing! The periods of the stretch and pendulum modes of oscillation are around 0.3 Hz.

The short term (1–10s) fractional frequency instability of the stabilized $\lambda = 282$ nm laser is reported by the NIST group to be less than 5×10^{-16}, compatible with the predicted shot noise limited stability of the detection signal in the present single mercury ion standard. The predicted limit to the fractional frequency instability of this standard is about $1 \times 10^{-15}\tau^{-1/2}$. In practice it is expected that the fractional instability is determined principally by fluctuations in the cavity for $\tau < 30$ s, and begins to behave as $\tau^{-1/2}$, as determined by the ion, only for longer times.

18.4.2 The Alkaline-Earth Single Ion Standards

These are proposed single-ion optical frequency standards based on $^{137}Ba^{+}$, $^{88}Sr^{+}$, and $^{40}Ca^{+}$. The singly charged alkaline earth elements have a single electron outside a closed shell structure with a $^{2}S_{1/2}$ ground state; the odd mass barium isotope has nuclear spin $I = 3/2$, whereas the even mass Sr and Ca have nuclear spin $I = 0$.

Interest in an ultra narrow quadrupole transition in $^{137}Ba^{+}$ as a possible optical standard has been reported by Norval Fortson's group at the University of Washington (Seattle). The work is primarily motivated by the search for possible drift in the fundamental constants of nature. The relevant energy levels of the $^{137}Ba^{+}$ ion are shown in Figure 18.8.

The clock transition is chosen to be the infrared $\lambda = 2051$ nm quadrupole transition between the metastable $5^{2}D_{3/2}(F' = 0)$ and the $6^{2}S_{1/2}(F = 2)$ ground state state. The upper state radiative lifetime is about 80 s, implying a line $Q > 10^{16}$, higher than any other ion candidate. The laser radiation for cooling and repumping at around the resonance transition wavelength $\lambda = 493$ nm, as well as for the clock transition can all be generated with solid state devices. The cooling wavelength is generated as the second harmonic of $\lambda = 986$ nm light from a diode laser/amplifier combination. The probe wavelength at $\lambda = 2051$ nm is generated by a diode-pumped Tm,Ho:YLF solid state laser.

Research on the $^{88}Sr^{+}$ ion as a potential candidate for an optical frequency standard has been reported by the groups at NPL (Britain) and NRC (Canada). As these are national standards laboratories, the optical standard aspect of the work on the strontium ion is naturally considerably more advanced than in the barium case. The choice by these laboratories of strontium over barium is presumably a

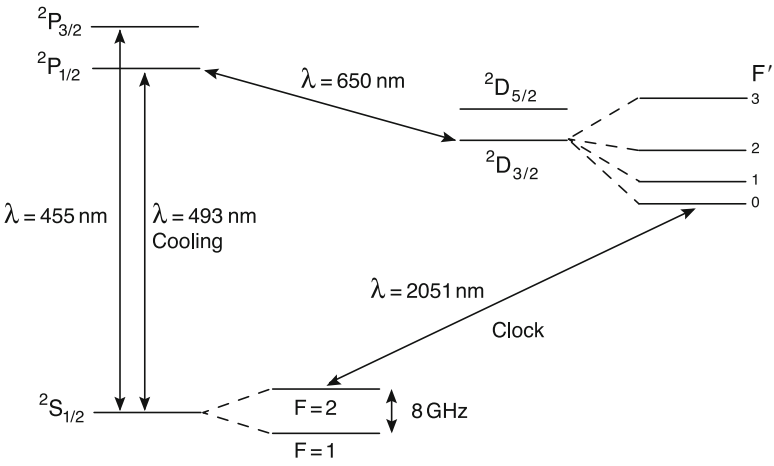

Figure 18.8 The relevant energy levels in $^{137}Ba^{+}$

compromise between extreme accuracy and ease of implementation: the strontium wavelengths are perhaps more easily realized using solid state lasers. Moreover to benefit from the much longer natural lifetime of its metastable state, the probe laser for barium would have to be much more stable.

The optical clock transition in $^{88}Sr^{+}$ is chosen to be at $\lambda = 674$ nm between the metastable $^{2}D_{5/2}$ and the ground state $^{2}S_{1/2}$, a transition that has a natural spectral width of about 0.4 Hz. A partial energy diagram for $^{88}Sr^{+}$ is shown in Figure 18.9. The even isotope of strontium has nuclear spin $I = 0$, so that there is no hyperfine structure in the energy levels, but of course in the inevitable presence of an external magnetic field there is Zeeman splitting of the energy terms. The upper state of the clock transition has a complex Zeeman structure with ten possible Zeeman components in the 674 nm clock frequency; therefore careful magnetic shielding of the earth's field is required and a uniform field of a few μT is introduced to resolve the Zeeman components. Cooling of the $^{88}Sr^{+}$ ion is carried out using the resonance transition $^{2}S_{1/2} \rightarrow {}^{2}P_{1/2}$ at $\lambda = 422$ nm generated as the frequency-doubled output of a laser diode system. A Nd^{3+} doped fiber laser is used as a repumper, driving the $\lambda = 1092$ nm transitions from the $^{2}D_{3/2}$ state back to the $^{2}P_{1/2}$ state. It is important to note that if repumping radiation maintains a particular polarization with respect to the magnetic field and beam direction it is possible to cause optical (Kastler) pumping into non-absorbing Zeeman sublevels in the $^{2}D_{3/2}$ state. The remedy is to rapidly rotate the polarization vector of the repumping beam using an electro-optic modulator. The primary source of the radiation probing the clock transition is a $\lambda = 674$ nm diode laser prestabilized and then locked to a high finesse ($F \approx 200{,}000$) fixed ultra-low expansion (ULE) cavity, temperature stabilized, *in vacuo*, free of vibration and mechanically isolated by suspension. To bridge the frequency interval between the clock frequency and the nearest mode of the ULE

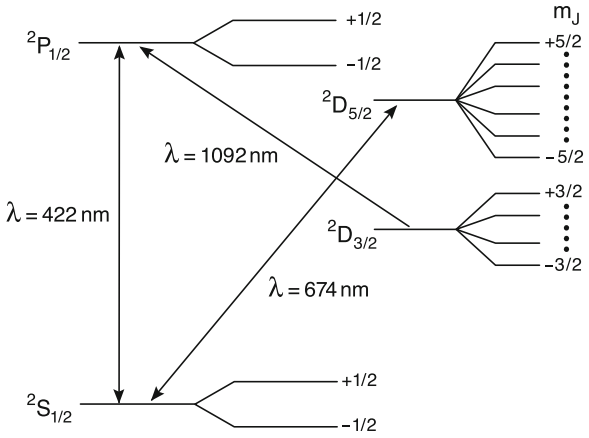

Figure 18.9 The relevant energy levels of $^{88}Sr^{+}$

cavity requires another "slave" extended-cavity diode laser that is modulated and a sideband locked to the master stabilized laser. By varying the modulation frequency the probe frequency can be tuned to the ion resonance. Otherwise, it is possible to shift the cavity-stabilized frequency by an electro-optic modulator to match the ion resonance. Probe laser line widths in the range of tens of hertz have been reported; with 20 ms interrogation pulse lengths, the ion resonance actually observed was about 100 Hz wide. Strontium has the drawback of having a linear Zeeman effect contributing to possible error in the determination of the center of the clock transition.

Finally we mention among the alkaline earth ions $^{40}Ca^{+}$ as a possible candidate, although its study in the past has been dedicated to it more in the context of quantum computing. Thus groups at CRL (Japan) and at U. Innsbruck (Austria) for example have reported work on this ion in which a single ion was cooled to the quantum ground state of vibration in a harmonic trap with a 99.9% probability. A miniature 3D Paul quadrupole trap was used operated with secular frequencies in the megahertz range, ensuring the ability to carry out sideband laser cooling.

18.4.3 The Indium and Ytterbium Single Ion Standards

A promising ion species that is expected to furnish an ultrahigh resolution reference optical frequency more immune from perturbations than all the other ions has been studied by Walther's group at the Max Planck Institute für Quantenoptik, (Garching, Germany). Of the ion species so far studied as possible optical frequency standards, the indium ion $^{115}In^{+}$, which has nuclear spin $I = 9/2$, is the only ion whose ground state has $J = 0$, nominally designated as $5s^2\ ^1S_0$, with a two-electron outer structure. The relevant energy levels are shown in Figure 18.10.

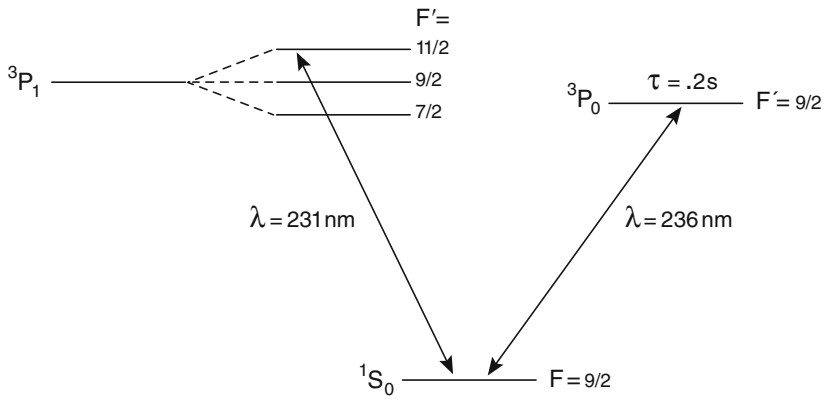

Figure 18.10 The relevant energy levels of $^{115}In^{+}$

There is a finite transition probability at $\lambda = 236.5$ nm from the $5s5p^3P_0$ state to the ground state, a transition proposed as defining the clock frequency. Were it not for the presence of a nuclear moment, this transition would be strictly forbidden; being between $J = 0$ states; it is through the intermediary of the nuclear hyperfine interaction that it happens at all. Because of that interaction, the $^3P_0$ state in fact does not have precisely the angular momentum number $J = 0$, but is a mixture of $J = 1$ states. The transition probability is of course small; but that is precisely what is called for in this case. The fact that the clock transition is between states that would have $J = 0$ were it not for a small perturbation, makes this ion uniquely immune to systematic frequency shifts due to electromagnetic fields, in particular static electric quadrupole shifts. The natural linewidth of the clock transition is about 8 Hz corresponding to a resolution of 6×10^{-16}.

The transition used for sideband cooling the ion is the resonance line between the ground state and the excited $5s5p^3P_1$ state at $\lambda = 230.6$ nm. This is a so-called *intercombination* line since it is between a singlet ($S = 0$) and a triplet ($S = 1$) state, involving a change in the electron spin state; the fact of its relatively large transition rate with a natural linewidth of 360 kHz is indicative of the approximate nature of the quantum state assignment.

The experimental procedure follows the now familiar technique of generating the probe beam by stabilizing a laser, in this case a diode pumped Nd:YAG non-planar ring laser to a Fabry–Pérot cavity using the Pound-Drever-Hall phase modulation technique, then quadrupling the frequency in non-linear crystals placed in field-enhancing cavities. Resonance detection is through the familiar double optical resonance ("electron shelving") method. A spectral resolution of 1.3×10^{-13} has been experimentally achieved by the Garching group, a figure limited by the stability of the probe laser.

Finally we consider the ytterbium ion $^{171}Yb^+$, a candidate that has been pursued by NPL (Britain) and PTB (Germany). The ion is attractive mainly because it has convenient wavelengths and offers a choice of more than one possible clock transition accessible with solid state lasers: in addition to a quadrupole transition to a $^2D_{5/2}$ state, similar to the $^{199}Hg^+$ ion, there is another quadrupole transition to a $^2D_{3/2}$ metastable state, and a much weaker octupole transition to a $^2F_{7/2}$ state. The ytterbium ion, like the mercury ion has nuclear spin $I = 1/2$; its relevant quantum levels are shown again for convenience in Figure 18.11. The quadrupole transition between the $6s^2S_{1/2}$ ($F = 0$) ground state and the $5d^2D_{3/2}$ ($F = 2$) excited state at $\lambda = 435.5$ nm is in the blue region of the spectrum and has a natural linewidth of 3.1 Hz.

The other quadrupole clock transition to the metastable $^2D_{5/2}$ has a wavelength $\lambda = 411$ nm. The clock transitions are chosen between $F = 0$ hyperfine components to avoid the linear Zeeman effect. Sideband cooling is achieved using the strong resonance transition between the alkali-like states $^2S_{1/2} \rightarrow {}^2P_{1/2}$ at $\lambda = 369.5$ nm. During the cooling phase repumping is required from the metastable states back to the $^2P_{1/2}$ state. The inordinately long life of the $^2F_{7/2}$ state would make clearing pulses essential in the detection cycle. The laser requirements

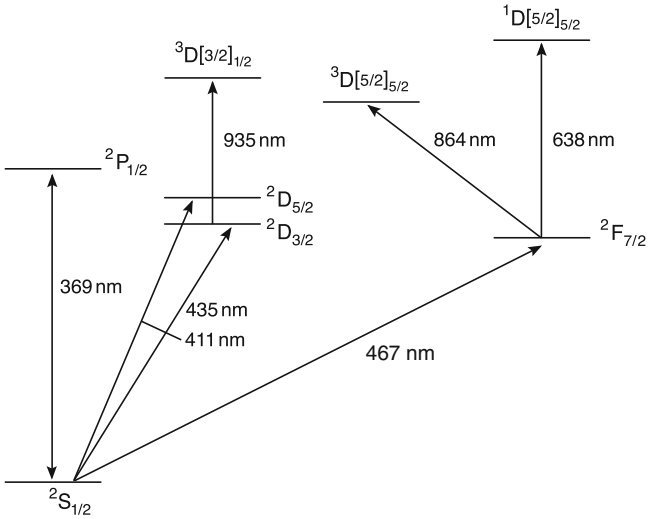

Figure 18.11 The relevant energy levels of $^{171}Yb^+$

are further complicated by the fact that each of these states has a complex hyperfine structure that must be addressed. Cooling of the ion can be achieved using the frequency-doubled output of a Ti:sapphire laser generating radiation at $\lambda = 738$ nm. If the octupole transition is to be used as the clock transition then a stable $\lambda = 467$ nm probe is required, which can be obtained by doubling the frequency of a stabilized $\lambda = 934$ nm Ti:sapphire laser. Experimentally the initial tuning to such a weak transition is no doubt a difficult challenge, requiring sophisticated spectroscopy.

18.4.4 Summary

We have reviewed the different ion species that are the subject of vigorous study in several laboratories around the world to evaluate their merit in providing a quantum transition of such constancy and sharply defined frequency as to serve as an optical frequency standard. A measure of the sharpness of the frequency is the line Q, which for optical frequency transitions in isolated ions *in vacuo* is many orders of magnitude larger than microwave transitions. Currently the highest observed line Q (1.5×10^{14}) has been reported for the 282 nm quadrupole transition in a single laser-cooled $^{199}Hg^+$ ion. The highest *theoretical* line Q is predicted for the very weak electric octupole transition in $^{171}Yb^+$ at 467 nm.

With the development of optical femtosecond pulse combs providing coherent frequencies over an octave of frequency that bridges the wide frequency interval between the optical and microwave regions of the spectrum, it becomes practical

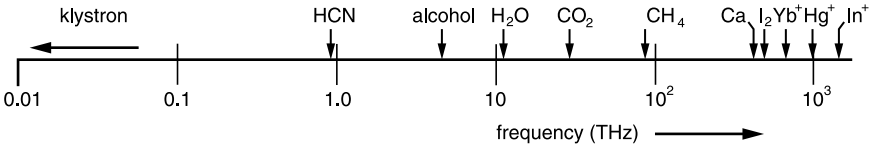

Figure 18.12 Available stabilized lasers plotted on a frequency scale extending from the microwave to the visible

to redefine the unit of time, the second, in terms of a very much more precise ion optical standard.

The field of horology is indeed going through a period of revolutionary change!

18.5 Optical Frequency Chains

Even given a series of highly stable and reproducible reference frequencies extending to the optical range, there remains the equally challenging problem of interrelating their frequencies and referring them back to the primary microwave standard. The classical procedure for making frequency comparisons is to mix the optical signals in a nonlinear device and measure the beat frequency between the higher frequency ν_2 and a harmonic of the lower frequency ν_1 according to the following:

$$\nu_2 - n\nu_1 = \nu_{\text{beat}}. \tag{18.1}$$

This is practical, provided that ν_2 and ν_1 are sufficiently stable and are such that a coherent low-frequency beat is observable, preferably within the microwave range. Optical frequencies are so high that even a small fractional deviation will lead to very large excursions in the beat frequency. Completing the chain of comparisons from the microwave standard to the optical range is made difficult by the wide gaps between the limited number of reference lasers, and their narrow tuning range. This is aggravated by the unavailability until recently of devices that can generate harmonics of sufficiently high order to bridge those gaps; in the microwave region it is possible to generate as high as the 1000th harmonic, whereas at infrared frequencies perhaps the 12th harmonic is possible. Even where a multiplicity of neighboring stabilized optical frequencies exists, the separations in frequency are still orders of magnitude larger than their tuning ranges.

This is demonstrated in Figure 18.12, where we have plotted on a *logarithmic* frequency scale (each unit is a *tenfold* increase) some of the established laser frequencies spanning the spectrum from the microwave to the visible.

18.5.1 The Point Contact MIM Diode

We recall that the generation of harmonics as well as the mixing of different frequencies to produce a sum or difference frequency is achieved using the nonlinear

response of certain devices. At microwave and lower frequencies, where the wavelength can be much larger than ordinary electronic components, the nonlinear device is a diode that can be treated as a *lumped* circuit element of negligible size. This is no longer possible when we reach the infrared region of the spectrum and beyond. Either we must find a device whose interaction with the light wave extends only over a microscopic region or failing that, take into account the oscillatory variation of the light wave across the device, that is, treat it as having a *distributed* interaction.

The most important nonlinear device responding to the "lumped" condition is the point contact metal–insulator–metal (MIM) diode. This is simply a finely etched tip of a tungsten wire in contact with the oxidized end surface of a nickel post, properly incorporated into a microwave circuit. These diodes respond to extremely high frequencies because the contact region has a diameter on the order of only $1/600$ the wavelength of the CO_2 laser. Moreover, the resistance and capacitance across the junction are relatively small, since electrons can tunnel through the nickel oxide film, which is only on the order of a few molecules thick. These MIM point contact diodes can mix and generate sum and difference frequencies of input light waves up to 200 THz ($\lambda = 1.5\,\mu\text{m}$) in the near infrared. Given two infrared frequencies whose *beat* (difference) falls in the microwave region of the spectrum, focusing them onto such a device mounted in a microwave circuit will produce a microwave output for further frequency measurement.

18.5.2 Optical Frequency Multiplication Chains

The pursuit of linking back the several isolated laser-stabilized optical frequencies with the microwave frequency of the primary Cs standard is as fundamental as that of gear trains in an analogous mechanical system. Until approximately the last decade, this took the form of frequency chains requiring a room full of dedicated, multiple laser systems, frequency mixers, harmonic generators, filters and phase lock loops (PLL). The result has been a number of successful determinations of optical frequencies based on different frequency chains. We can distinguish two different approaches to constructing the frequency bridges: one can be described briefly as the frequency multiplication method and the other, the more useful frequency division method.

Although the multiplication chains differ in the detailed way in which phase coherence and stability are transferred from one member of the chain to the next, they are for the most part based on the harmonic generation principle already mentioned. Each link in the chain involves a *phase-lock loop* of some sort, that is, a servo loop in which the phase difference between the beat signal derived from a mixer and a synthesized (relatively) low frequency constitutes the error signal, properly conditioned, so that apart from the synthesized frequency offset, the phase of one laser is locked to a harmonic of the other. While this approach has been

successfully applied to linking a specific optical frequency, such as that of a stabilized He–Ne laser to the microwave standard using a particular frequency chain, the narrow tuning range of lasers makes it difficult to apply to the measurement of arbitrary optical frequencies.

For a clock based on an optical frequency standard, it would be at present necessary to determine the frequency of the chosen optical standard in terms of the primary microwave Cs standard. As an illustrative example of one such frequency chain developed in the past at the Physikalisch-Technische Bundesanstalt, is illustrated in Figure 18.13 Currently there are much more powerful techniques for frequency comparisons, which we take up later in this chapter.

18.5.3 A Frequency Division Chain

There are more recent approaches, based on a more powerful *frequency division* principle. In the first, it is not actually the frequency itself that is divided, but rather at each stage in the chain there is a division by two of the frequency *difference* between two laser signals. If at some point in the chain the two frequencies whose difference is to be divided by two are ν_1 and ν_2, then the idea is to generate using nonlinear elements the frequency $^1/_2(\nu_1 + \nu_2)$. This and the frequency ν_2 differ by $^1/_2(\nu_1 - \nu_2)$; that is, we now have two frequencies that differ by half the original

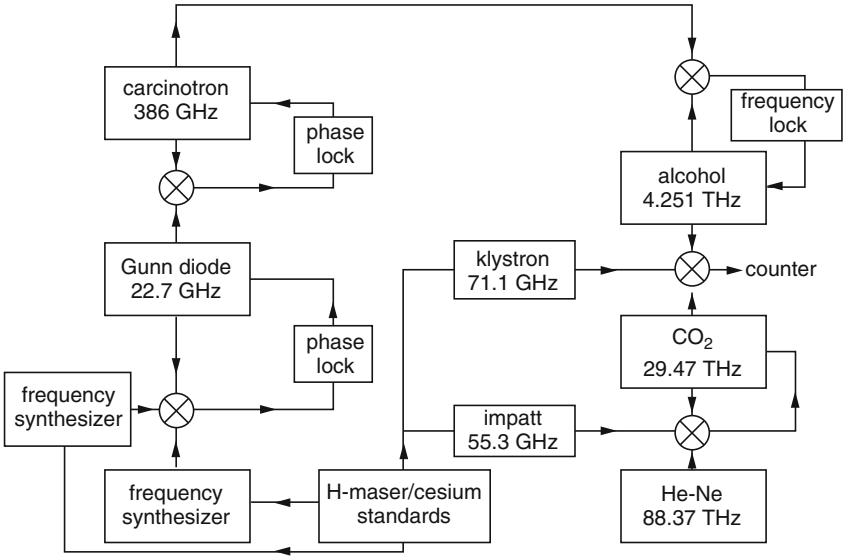

Figure 18.13 A frequency chain of the Physikalisch–Technische Bundesanstalt (Kramer, 1992)

difference. If the process is repeated, the frequencies will differ less and less until their beat frequency falls in the microwave range and can be compared directly with the primary standard. The original difference in frequency at the top of the chain can then be calculated; that difference may in fact be the frequency of the optical standard itself, simply by taking the other frequency as its second harmonic.

Another noteworthy approach to linking optical to microwave frequencies exploits the frequency-dividing property of optical *parametric* oscillators (OPO). The concept of a parametric excitation of an oscillator has already been encountered: We recall the mechanical example of the "pumping" of a swing. It occurs whenever a parameter, such as the "spring constant," controlling the resonant frequency of an oscillatory system is modulated at certain frequencies. In the optical case, a modulation of an optical parameter of a medium, such as its refractive index, can occur if the medium is nonlinear, and an intense optical wave, called the *pump,* interacts with it. This can lead to the excitation of optical fields at two other frequencies called the *signal* and *idler* waves, which must satisfy the following conditions on their frequencies and wave vectors:

$$\nu_3 = \nu_1 + \nu_2; \mathbf{k}_3 = \mathbf{k}_1 + \mathbf{k}_2, \tag{18.2}$$

where the indices 1, 2, 3 designate the signal, idler, and pump waves, respectively. These have the general form of the conditions we have already encountered as the *phase* conditions in the case of second-harmonic generation, which we would get in the so-called *degenerate* case when the signal and idler waves are one and the same. There is an important difference, however. Here the applied pump beam has twice the frequency of the excited signal/idler beam; that is, a wave has been produced at *half* the frequency of the pump beam, and not one at the second harmonic. This is the basis, then, for optical frequency division, provided that high quality nonlinear crystals and stable high-power laser sources are available to act as pumps.

Optical parametric division was demonstrated in 1992 by N.C. Wong and D. Lee at MIT (Wong, 1992) using a biaxial KTP crystal in a doubly resonant cavity configuration in which both the signal and idler waves are resonant at slightly different frequencies. The signal at the beat frequency between the signal and idler waves ($\nu_1 - \nu_2$) is phase-locked to a microwave reference frequency (ν_μ), so that from the known pump frequency ν_3 are produced two precisely known frequencies given by

$$\nu_{1,2} = \frac{\nu_3}{2} \pm \frac{\nu_\mu}{2}. \tag{18.3}$$

Since ν_μ is much smaller than the pump frequency, this constitutes a 2:1 frequency divider stage. It is important to note that the signal and idler wave *phases* are constrained to obey the condition $\phi_3 = \phi_1 + \phi_2$, and that since the phase of the beat signal is phase-locked to the microwave reference source, the output waves are phase

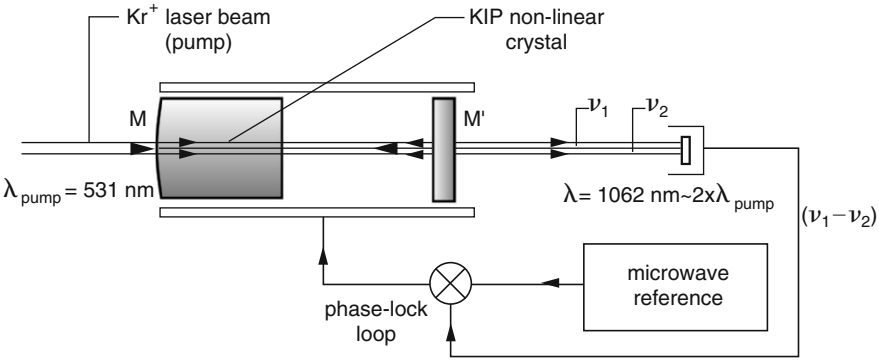

Figure 18.14 Optical frequency division using parametric oscillators (Wong, 1992)

coherent with the pump wave. In the actual experiment, illustrated in Figure 18.14, Lee and Wong used the output of a Kr^+ ion laser at $\lambda = 531$ nm as the pump to generate infrared signal and idler beams at approximately the degenerate value of $\lambda = 1.06\,\mu$m. The corresponding threshold power for parametric oscillation was around 40 mW. The KTP crystal, 8 mm in length, was placed in an optical cavity made up as follows: At one end the surface of the crystal itself had a radius of curvature of 40 mm and was coated to provide maximum reflectance at the infrared wavelengths; at the other end was the output mirror, coated to have a 0.5% transmittance. On the other hand, the optical coatings of the reflecting surfaces were chosen so that the green pumping beam enters the cavity through the crystal and is reflected back by the output mirror at the other end through the cavity. The frequency separation of the two output infrared beams could be varied by about 1 THz by changing the angle of incidence of the pump beam with respect to the crystal. A piezoelectric crystal drive attached to the output mirror controlled the cavity length, and different mode pairs of signal and idler could be brought into resonance.

The application of this technique in a serial fashion, in which an optical frequency is sequentially divided by two until a microwave frequency is reached, suffers from loss of power on each conversion and the need for high efficiency through the far infrared region of the spectrum. A clever alternative *parallel* scheme of conversion stages has been proposed by Lee and Wong, in which the same optical pump source is used to drive a parallel set of parametric oscillators whose signal–idler frequency separation increases in a regular progression. In this way a very wideband frequency comb spanning the spectrum between chosen (rational) fractions of the pump frequency is generated. Each frequency in this comb is further split into finer "secondary" combs by phase modulation driven by a reference microwave source. The scheme promises to provide the means of synthesizing the full range of coherent optical frequencies derived from an optical reference standard.

18.6 Optical Frequency Comb Generators

18.6.1 Intracavity Modulation

An interesting optical frequency synthesis device involves the generation of a multi-THz wide frequency comb using a CW single frequency laser source locked to an optical cavity in which a microwave electro-optic modulator (EOM), driven at a multiple of the cavity mode separation, phase locks the longitudinal modes, a condition reminiscent of a mode-locked laser. The cavity resonance enhances the efficiency of the modulator and thereby ensures the build up not only of the mode resonant with the laser but also the sideband longitudinal modes. At the modulation index $\Delta\nu/\nu_0$ typical in practice the EOM generates principally the first order resonant sidebands, which in turn produce their own sidebands, and so on extending the frequency comb until a limit is reached depending on the modulation index and the finesse of the cavity. Figure 18.15 shows schematically the layout of an optical frequency comb generator.

A number of interesting frequency comparisons have been made using this device to bridge frequency gaps as large as 1.78 THz; for example between the Cs resonance line at 852 nm and the fourth harmonic of methane stabilized He–Ne laser. This is probably near the limit of the bandwidth practicable with this design, set by practical limits of modulation index, finesse and optical dispersion in which differences in the phase velocity of different frequency modes become significant. The drive to reach wider bandwidths ultimately led in the last few years to a number of refinements, the most notable being the use of parametric gain in a non-linear crystal, which is incorporated into a parametric oscillator cavity together with an electro-optic modulator to generate a comb of sidebands.

Such attempts however have been overtaken by recent revolutionary advances in the field of mode-locked lasers, which we outline in somewhat more detail below.

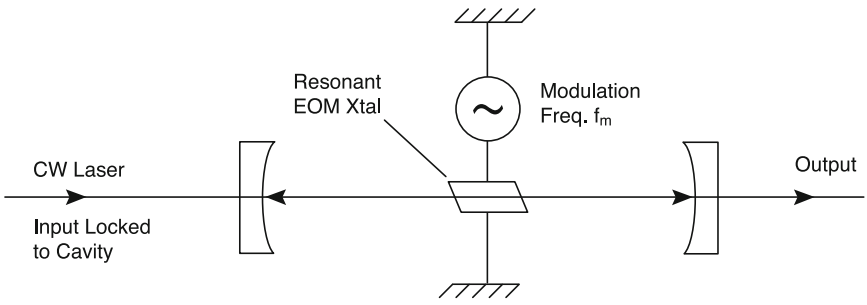

Figure 18.15 Intra-cavity EOM comb generator

18.6.2 Kerr Lens Mode (KLM) Locking Technique

We saw at the end of Chapter 14 how a laser may oscillate simultaneously in many longitudinal modes that can extend over a very wide frequency range in certain amplifying media, and how they may be locked to a common phase. We may describe such a mode-locked output equivalently in the time domain as a train of short pulses or, through the Fourier transform, as having a frequency spectrum consisting of equally spaced lines separated by the *free spectral range* of the loaded optical cavity, that is, on the order of $c/2n_rL$. Such a spectrum of equally spaced lines is called a frequency *comb*. Mode locked lasers as generators of wide frequency combs have several advantages: among these are: (1) they have a spectral span that can equal a full octave (a factor of two in frequency), and (2) they do not require the active tuning of a modulator frequency to cavity resonance; ultra-short pulses result from all modes being phase locked simultaneously.

The earliest application of the frequency comb generated by a mode-locked dye laser was to two-photon transitions in sodium reported back in 1978 by Hänsch and his coworkers. However it was not until around 1991 that a transforming development in the field occurred with the development by Sibbett, et al. at St Andrews University (Sibbett, 1991) of the Kerr-lens-mode-locked (KLM) Ti:sapphire laser, which, when combined with the use of the so-called *photonic crystal fibers* proved ultimately in the hands of Hänsch and his group at the Max Planck Institut für Quantenoptik capable of generating a frequency comb spanning a full octave. Following this breakthrough came a flood of activity exploiting this type of device.

It owes its remarkable success mainly to two factors: (1) the Kerr lensing effect which in effect can be made to favor, in terms of laser gain, high intensity fields in the cavity without the limitation of a finite recovery-time that saturable absorbers have, and (2) effective means of correcting for optical dispersion, which limits the extent of the comb because the different constituent (Fourier) frequencies (or modes) propagate with slightly different velocities, with ultimate loss of coherence.

Before discussing the KLM Ti:sapphire laser further it may be useful to recall the optical Kerr effect. First we should distinguish between the optical frequency Kerr effect and the old fashioned static field effect as exploited in the Kerr cell shutter. In the latter, a constant or low frequency electric field is applied to an optical medium, inducing birefringence similar to a uniaxial crystal with the optic axis parallel to the field direction. The amount of induced birefringence as measured by the difference between the refractive indices $(n_o - n_e)$ is proportional to E^2. This quadratic dependence on the field is somewhat misleading because it is really a third order effect when described in terms of the induced electrical polarization. Because the induced *polarization* is not a quadratic function of the electric field, the effect can be observed in varying degrees in *any* crystal, even those that have a center of symmetry. Nitrobenzene has an unusually large Kerr constant, while different types of glass have values that vary widely, the largest being on the order of $3 \times 10^{-14}\,\mathrm{cmV}^{-2}$. On the other hand, the so-called "linear" electro-optic effect (the Pockels effect) is *not* present in crystals with a center of symmetry since the

change in polarization (not the refractive index) *is* in fact a quadratic function of the electric field. As for the optical Kerr effect, as it relates to the propagation of an optical frequency wave, we are confronted with the complex field of non-linear optics in which it is most useful to work in the frequency domain, involving the (Fourier) spectral densities of the field quantities.

The essential fact that makes Kerr lens mode locking possible is that the optical field amplitude in a laser cavity is maximum along the axis, falling off rapidly away from it, generally following a Gaussian function. Such a field distribution in a medium such as Ti:sapphire, that exhibits the Kerr effect, the optical wavefront will travel slower along the axis than the periphery, causing the wavefront to converge toward the axis, exactly as if it were passing through a convex lens. Since the change in refractive index increases with intensity, the tighter the convergence the more it is reinforced. This can lead to mode locking under two circumstances: (1) the effective presence of a "soft" aperture, or (2) the insertion of an actual beam limiting "hard" aperture. The first exists if the Ti:sapphire crystal is optically pumped by a laser beam narrowly concentrated along the crystal axis, then the convergence produced by the Kerr effect on the laser field increases the overlap with the pumping beam and hence the optical gain. On the other hand a physical aperture appropriately placed in the cavity to absorb all radiation beyond a fixed radius would again favor the build up of high intensity fields through phase locking of what would otherwise be randomly phased longitudinal modes. From the initial condition in which the optical field appears to fluctuate randomly in time with highs and lows where some modes happen to reinforce or cancel each other, the occurrence of a momentary high will, through the Kerr lens effect, make the modes favor being in phase to produce an even stronger Kerr focus. This ultimately leads to the phase locking of all the modes and an output consisting of a succession of sharp laser pulses at equal time intervals.

The basic elements of a mode-locked Ti:sapphire laser are shown schematically in Figure 18.16. The design is the standard four-mirror Z-folded resonator, with focusing spherical mirrors and two arms bounded by plane mirrors, one of which is partially transmitting, labeled OC, the output coupler. If the effective distance D between the two focusing mirrors M_1 and M_2, of focal lengths f_1 and f_2, is written as $D = f_1 + f_2 + \delta$, the quantity δ is an important stability parameter.

As D is varied, the laser CW oscillation power level goes through two separate maxima, corresponding to stability zones, a consequence of the asymmetry between the optical path lengths of the two arms of the cavity M_1-OC and M_2-CM; Kerr lens mode locking usually starts in a particular range of δ.

To achieve output pulse widths approaching the femtosecond range it is necessary to compensate for optical dispersion. We have already mentioned the use of chirped multilayer dielectric mirrors for that purpose; another popular technique is to exploit the dispersive property of a prism. The design calls for two prisms arranged in such a manner that the optical path length through them is greater for the red end of the spectrum than the blue, that is, the red wavefront is delayed with respect to the blue, corresponding to what is defined as *negative* dispersion, since

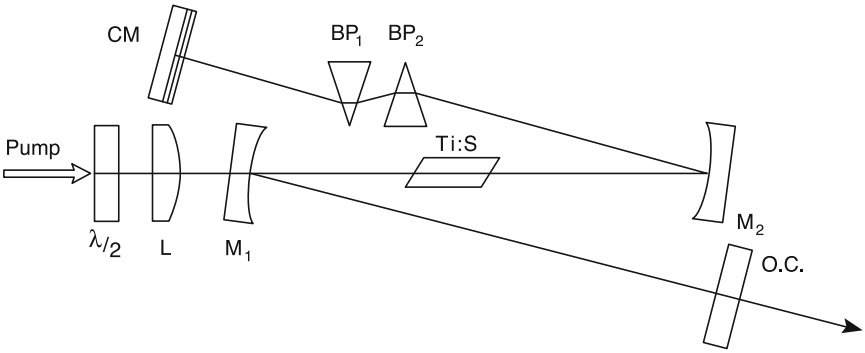

Figure 18.16 Schematic diagram of the layout of a mode-locked Ti:Sapphire laser. The chirped mirror (CM) and the Brewster prisms (BP) provide phase dispersion correction and OC is the output coupler

the more common reverse dispersion in media such as glass is defined as positive. Proper compensation for the *group delay dispersion* in the system requires that the distance between the prisms be correctly adjusted. The prisms are set at minimum deviation with the beam incident at the Brewster angle to minimize loss.

18.6.3 Absolute Determination of Optical Frequencies.

A radical simplification in the measurement of optical frequencies in terms of the microwave Cs standard was demonstrated in a collaboration between NIST, Bell Labs and Max Planck Inst. f. Quantenoptik in the year 2000 (Diddams et al., 2000). It was accomplished by a combination of the femtosecond Ti:sapphire laser techniques and new developments in optical fiber technology involving the use of microstructures. The frequency of an iodine-stabilized Nd:YAG laser at about 282 THz ($\lambda = 1064$ nm) was measured directly in terms of the microwave separation of the comb frequencies.

In a microstructure fiber what would normally be a continuous dielectric cladding surrounding the core is in fact one in which there is a regular array of holes running the length of the fiber; for that reason it is also sometimes referred to as *photonic crystal fiber* (PCF) (the use of the word "crystal" here is only meant to suggest the periodic variation in the refractive index that the hole structure creates). In Figure 18.17 is shown a cross section of such an air-silica microstructure fiber.

The two properties that these optical fibers have that are key to making the *direct* comparison of optical and microwave frequencies possible are: (1) the enormous peak intensity of the pulsed laser field along the fiber core generating high order nonlinear effects such as harmonic generation, frequency mixing, Raman scattering, etc., and (2) the possibility of designing the air-silica microstructure so that a single mode is propagated, and (3) being able to shift the wavelength at

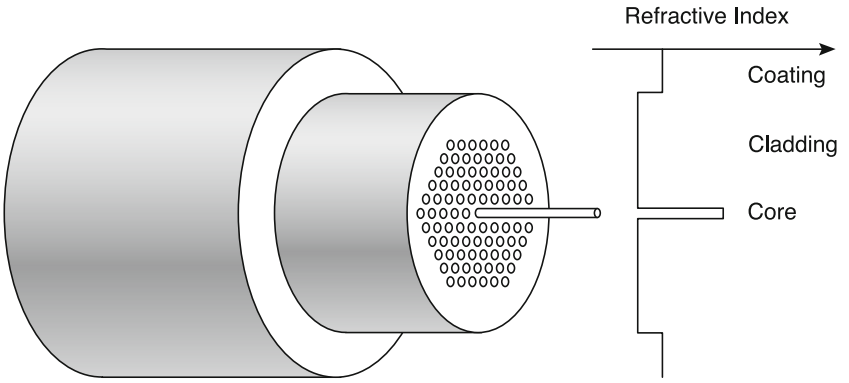

Figure 18.17 Cross section of an air-silica microstructure optical fiber

which the phase dispersion is zero to a desired optimum value. It was by exploiting these design capabilities that the frequency comb generated by a Ti:sapphire mode-locked laser was ultimately broadened to cover an entire optical octave. This is a critical step. Such a comb provides a frequency yard stick whose "units" can be referred to the primary microwave standard, a yard stick that extends from the given unknown frequency to twice that same frequency produced in a nonlinear crystal.

In the 2000 paper cited above, the air-silica microstructure fiber had a diameter of only about 1.7 μm, and the group velocity dispersion was designed to occur at $\lambda = 800$ nm; this ensured that the time-spreading of pulses was minimized and the peak intensities, reaching hundreds of GW/cm^2, were maintained over a substantial distance along the fiber. This is important since the optical nonlinearity of silica is not particularly large, and spectral broadening through self-phase modulation due to an intensity dependent refractive index, requires a substantial interaction length. Figure 18.18 shows the extent to which the band width of the output from the microstructured fiber is increased.

Their KLM Ti:sapphire laser had a frequency centered at around 800 nm with output pulses about 10 fs wide. The (loaded) cavity length was such that the output pulse train had a Fourier frequency comb of $f_m = 100$ MHz spacing. This was stabilized by controlling the laser cavity length with a piezoelectric transducer (PZT) to phase lock the 100$^{\text{th}}$ harmonic of f_m to a stabilized 10 GHz source, whose internal clock was referred to a local rubidium standard. As this work was carried out co-operatively between groups on opposite sides of the Atlantic Ocean, the frequency offset of the local rubidium standard was referred back to the NIST cesium standard clocks by means of a common-view GPS time comparison, incidentally testing the uncertainties in international time dissemination using GPS.

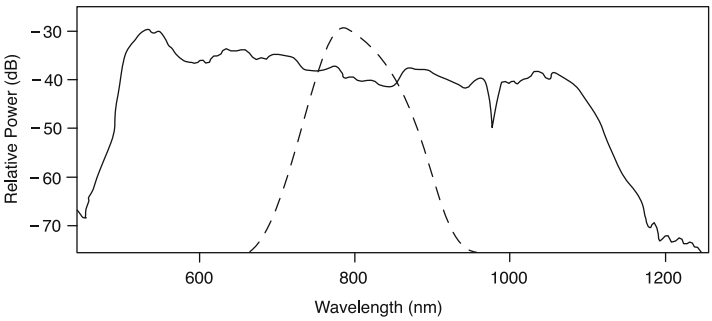

Figure 18.18 The dotted curve represents the power spectrum of the direct output of the Ti:sapphire laser; the solid curve the output from the fiber (Diddams et al., 2000)

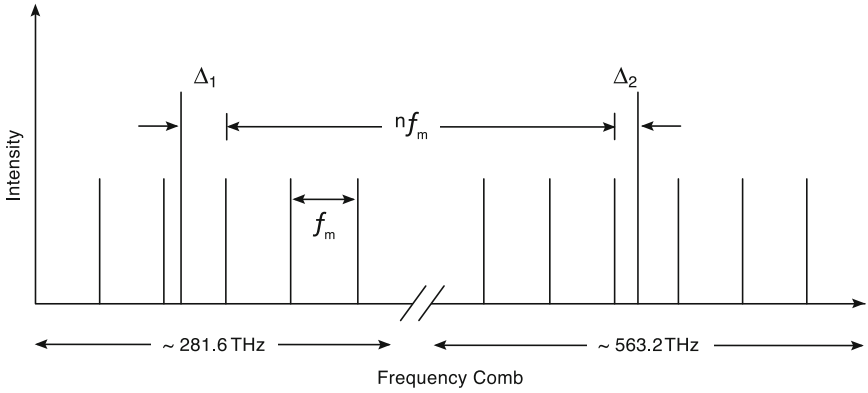

Figure 18.19 The spectrum of the I_2-stabilized Nd:YAG frequency combined with its second harmonic and the frequency comb generated by the Ti:sapphire laser/crystal fiber

To determine the absolute frequency of the iodine-stabilized Nd:YAG laser ultimately in terms of the NIST Cs standards, the procedure consists of the following: (1) the fundamental frequency output of the Nd:YAG laser at $\lambda_1 = 1064$ nm is frequency doubled to yield $\lambda_2 = 532$ nm., (2) these two wavelengths are combined and mode-matched with the output of the femtosecond pulse output of the fiber, (3) the three beams are wavelength-dispersed by a grating, and (4) the rf beat frequency Δ_1 (Δ_2) between each wavelength $\lambda_1(\lambda_2)$ and its nearest "tooth" of the frequency comb are detected with fast photodiodes. The measurement of only a beat frequency between two frequencies does not, of course, by itself establish which frequency is greater (or less) than the other. The situation is made clearer by reference to Figure 18.19. To resolve the ambiguity, assume the Nd:YAG laser cavity length is constant, then any perturbation that causes the comb position to shift on the frequency scale will not affect the *sum* of the beat frequencies Δ_1 and

Δ_2 if the Nd:YAG frequency and its second harmonic are on *opposite* sides of their adjacent "teeth" in the frequency comb. Similarly the difference would not be affected if they are on the same side. In fact, by comparing the fluctuations observed in the sum and difference of the beat frequencies it was concluded that the sum is appropriate, and having prior knowledge of the Nd:YAG wavelength to within 20 kHz, much less than the comb spacing, the remaining ambiguity was resolved by trying different values of n.

The final measured value for the I_2-stabilized Nd:YAG frequency under study was given as 17.2 kHz higher than the value given by the Comité International des Poids et Mesures (CIPM), with a statistical uncertainty of about 2×10^{-13}.

Since the technical breakthrough by Hänsch and his group that we have just described, the method has been applied to the absolute determination of the frequency of several other candidates for optical standard. Most notable are the work on $^{199}Hg^{+}$ by the NIST group, on $^{88}Sr^{+}$ at NPL and $^{171}Yb^{+}$ at PTB. The frequency of the proposed transition in the mercury ion has been measured by the NIST group relative to the Cs fountain standard with the result given as (Udem et al., 2001):

$$f(Hg^{+}) = 1{,}064, 721, 609, 899, 143(10)\ \text{Hz}$$

The fractional statistical uncertainty in this value is about 9×10^{-15}! More recently (Tanaka 2003) a systematic evaluation of an optical $^{199}Hg^{+}$ standard was carried out using a second similar standard over a period of 21 months; the variation in frequency was found to be less than one part in 10^{-14}.

The measurement on the strontium ion by NPL is reported to be approximately three times more accurate. Clearly the accelerated pace of development of optical standards has brought closer the day when precision time will be measured with an optical clock and the official unit of time, the second, will be defined in terms of oscillations at optical frequencies.